Friction
https://doi.org/10.1007/s40544-023-0846-3
ISSN 2223-7690
CN 10-1237/TH
RESEARCH ARTICLE

Exploring the relevance between load-bearing capacity and surface friction behavior based on a layered hydrogel cartilage prototype

Yunlei ZHANG[1,2], Weiyi ZHAO[1,2], Xiaoduo ZHAO[1], Jinshuai ZHANG[3], Bo YU[1], Shuanhong MA[1,3,*], Feng ZHOU[1,*]

[1] *State Key Laboratory of Solid Lubrication, Lanzhou Institute of Chemical Physics, Chinese Academy of Sciences, Lanzhou 730000, China*

[2] *College of Materials Science and Opto-Electronic Technology, University of Chinese Academy of Sciences, Beijing 100049, China*

[3] *Shandong Laboratory of Yantai Advanced Materials and Green Manufacture, Yantai Zhongke Research Institute of Advanced Materials and Green Chemical Engineering, Yantai 264006, China*

Received: 4 September 2023 / Revised: 16 October 2023 / Accepted: 11 November 2023

Abstract: Cartilage is well lubricated over a lifetime and this phenomenon is attributed to both of the surface hydration lubrication and the matrix load-bearing capacity. Lubricious hydrogels with a layered structure are designed to mimic cartilage as potential replacements. While many studies have concentrated on improving surface hydration to reduce friction, few have experimentally detected the relationship between load-bearing capacity of hydrogels and their interface friction behavior. In this work, a bilayer hydrogel, serving as a cartilage prototype consisted of a top thick hydrated polymer brush layer and a bottom hydrogel matrix with tunable modulus was designed to investigate this relationship. The coefficient of friction (COF, μ) is defined as the sum of interfacial component (μ_{Int}) and deformation/hysteresis component (μ_{Hyst}). The presence of the top hydration layer effectively dissipates contact stress and reduces the interface interaction (μ_{Int}), leading to a stable and low COF. The contribution of mechanical deformation (μ_{Hyst}) during the sliding shearing process to COF can be significantly reduced by increasing the local mechanical modulus, thereby enhancing the load-bearing capacity. These results show that the strategy of coupling surface hydration layer with a high load-bearing matrix can indeed enhance the lubrication performance of hydrogel cartilage prototypes, and implies a promising routine for designing robust soft matter lubrication system and friction-control devices.

Keywords: soft contact; hydration, deformation; load-bearing; friction control

1 Introduction

Articular cartilage remains well lubricated throughout a lifetime under harsh loading condition [1–4]. The low coefficient of friction (COF) of cartilage has been attributed to the synergy from its good surface hydration lubrication and the considerable load-bearing capacity supported by synovial fluid pressurization and gradient biochemical structure [4–9]. Hydrophilic proteoglycans and phosphatidylcholine lipids anchoring at the surface layer act as good boundary lubricants for achieving hydration lubrication[1], while the gradient cartilage matrix constituted by different oriented collagen fibers serve as load-bearing layer, supporting the tangential and normal stress (Fig. 1(a)) [5, 10]. Synthetic hydrogels, desighed as potential replacements, aim to imitate natural cartilage [11–15]. Based on the hydration lubrication mechanism of cartilage, surface functionalized hydrogels with biomimetic layered structure have been designed, and hitherto many efforts have been devoted to improve the surface lubrication performance of cartilage-inspired hydrogels [1, 4, 9, 16–20]. However, the inherently poor mechanical properties of traditional

* Corresponding author: Shuanhong MA, E-mail: mashuanhong@licp.cas.cn; Feng ZHOU, E-mail: zhouf@licp.cas.cn

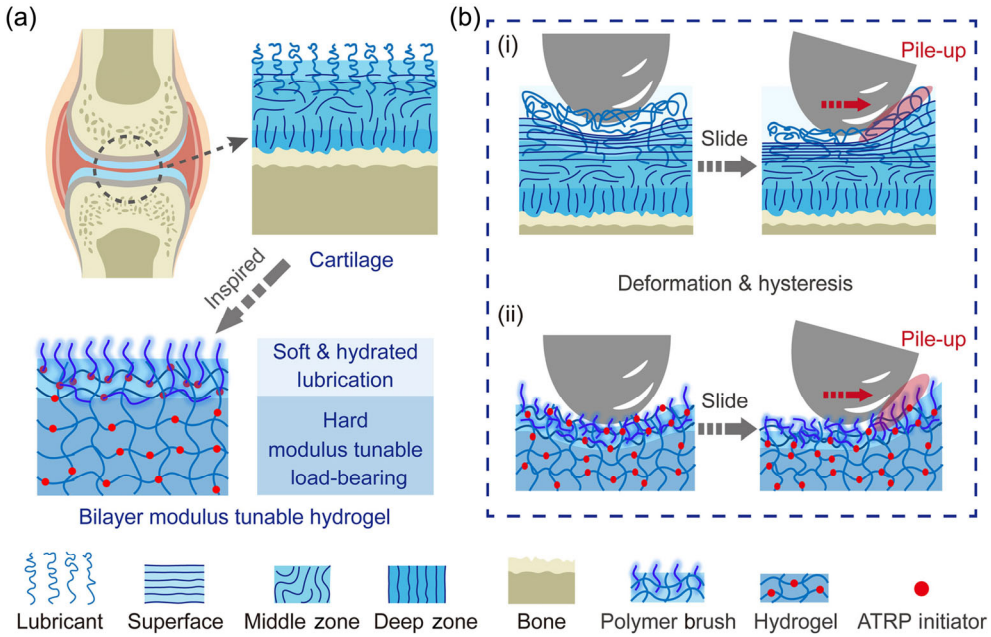

Fig. 1 (a) Schematic diagram of an articular cartilage and corresponding schematic diagram of the bilayer modulus tunable hydrogel (BMTH). (b) Schematic illustration of the deformation and hysteresis contribution in loading and sliding process of (i) articular cartilage and (ii) hydrogel.

hydrogels commonly induce large deformation under dynamic loading/shearing [9, 21, 22]. Meanwhile, the viscoelasticity of hydrogel is typically pronounced enough to make the influence of deformation/hysteresis be more prominent in the contribution of whole friction process [9, 21–23]. According to the coupling strategy of the sliding cartilages interface, a low COF requires that hydrogels not only have a highly hydrated surface (interface contribution), but also an excellent load-bearing capacity to minimize deformation/hysteresis and pile-up during sliding/plowing (deformation/hysteresis contribution) (Fig. 1(b)) [24–28]. Although many strategies were developed to enhance the mechanical toughness of hydrogels and improve their load-bearing capacity [29–39], it often results in a decreased surface hydration lubrication effect [9]. Therefore, the development of hydrogels-based cartilage prototype to balance hydration and load-bearing functions has become a challenge. Some cartilage-inspired layered hydrogels and lubricant-mixed hydrogels with strong load-bearing capacity have been developed recently to improve the poor surface lubrication performance of tough hydrogels [40–43]. Correspondingly, mechanism studies focusing on surface hydration-dominated frictional behavior of hydrogel cartilage prototypes have revealed its richness and complexity, but few focuse on experimentally investigating the deep relationship between load-bearing capacity of hydrogel matrix and friction behavior systematically, which greatly limits the development of robust hydrogels cartilage materials.

In this work, a bilayer modulus tunable hydrogel (BMTH) as novel cartilage prototype consisted of a top thick hydration layer from hydrophilic polyelectrolyte brush and a bottom matrix with tunable moduli were designed to systematically investigate the relationship between load-bearing and friction. The top soft and hydrated layer showed excellent lubricity and dissipation of contact stress, whereas the bottom modulus tunable hydrogel matrix contributes to the load-bearing capacity. By tuning the mechaincal moduli of bottom matrix, a series of BMTH samples with different load-bearing capacities were obtained to explore the relationship between load-bearing capacity and lubrication. Experimental results showed that the bottom modulus tunable hydrogel (MTH) matrix with good load-bearing capacity can effectively reduce the influence of deformation/hysteresis in friction process, thus obtaining lower COF. By contrast, BMTH, which couples the lubrication layer with a strengthening matrix, demonstrated both of lower COF and superior anti-wear properties. These results

show adopting the strategy of coupling robust surface hydration and strengthening mechanics of hydrogel matrix can indeed enhance the lubrication performance of cartilage-inspired hydrogels, and implies a promising rountline for designing intelligent soft matter lubrication system.

2 Materials and methods

2.1 Materials

Acrylic acid (AA, >99%, TCI, Japan), acrylamide (AAm, >99%, J&K Chemical Ltd., China), N, N′-methylene diacrylamide (MBAA, >99%, Sinopharm Chemical Reagent Co. Ltd., China), Calcium acetate ($C_4H_6CaO_4$, >99%, Tianjin Chemical Reagents Corp., China), α-ketoglutaric acid (99%, J&K Chemical Ltd., China), 2-hydroxyethyl methacrylate (HEMA, 99%, J&K Chemical Ltd., China), 3-sulfopropyl methacrylate potassium (SPMA, >99%, TCI, Japan), sodium carbonate (Na_2CO_3, >99%, Sinopharm, China), sodium chloride (NaCl, >99%, Sinopharm, China). Dichloromethane and anhydrous methanol were purchased from Tianjin Chemical Reagents Corp., China. Dichloromethane was dried over CaH_2 before use. 2,2′-Bipyridine (Bipy, 99%) and copper (I) bromide (CuBr, 99%) were purchased from TCI Co., Ltd., Japan. CuBr was purified by stirring overnight in acetic acid.

2.2 Preparation of hydrogels

Preparation of P(AAc-co-HEMA-Br) hydrogel: The SSI-ATRP initiator was synthesized from a previously described procedure [25]. The composite PAAc hydrogel with SSI-ATRP initiator was synthesized via two steps. First, monomer of AAc (2.16 g, 30 mmol), initiator of α-ketoglutaric acid (10 mg, 0.068 mmol), crosslinker of MBAA (23 mg, 0.15 mmol), HEMA-Br initiator(3% mass ratios of AAc) were added in 10 mL pure water to obtain homogeneous solution. After being vigorously stirred for 10 min with gassing nitrogen, the resulting solution was subjected to UV irradiation for photo-initiators for 4 h to form a covalently crosslinked hydrogel. Then, the covalently crosslinked hydrogel was immersed in the CaAc solution (250 mM) for 2 weeks to form the AAc-CaAc network.

Synthesis of PSPMA brush-grafted hydrogels: Polymer brushes were grafted from initiator embedded composite hydrogel substrate by ATRP technique. The typical polymerization process was as follows. The monomer, SPMA (6 g, 24.4 mmol) was dissolved in the 8 mL water and 4 mL methanol at room temperature and degassed for 30 min with N_2. And then, the 2,2′-bipyridine (80 mg, 0.512 mmol) and CuBr (35 mg, 0.244 mmol) were added in this solution. The mixture was further stirred and degassed with N_2 for another 20 min. The composite hydrogel sheet with 3 M tape protected on side was put into the reaction solution under N_2 protection without being stirred for a certain period (10, 15, 20, 30, 40, 60, and 90 min). Finally, the samples were taken out and washed with deionized water to remove any unreacted monomers and catalysts.

Synthesis of MTH and BMTH: The P(AAc-co-HEMA-Br) hydrogel (MTH) and P(AAc-co-HEMA-Br)-B hydrogel (BMTH) were immersed in the CaAc solution with different concentrations (250, 500, 750, 920, 960, 1,000, 1,200, 1,400 mM) to form different CaAc-AAc network.

2.3 Characterizations

Mechanical properties measurement: The mechanical properties were measured using an electrical universal material testing machine with a 500 N load cell (EZ-Test, SHIMADZU, Japan). The testing velocity was kept at 20 mm/min for tensile measurement. The sample was cut into sheets (size: 50 mm × 5 mm × 1 mm).

Rheometry test: The viscoelastic properties of the hydrogels immersed in different CaAc solutions were analysed with rheometer (RS6000, HAAKE, Germany). A gel disc 20 mm in diameter was used for test. A small amount of CaAc solution was added to the platform to prevent the sample from drying. Measurements of the storage (G′) and loss (G″) moduli were carried out from 0.1 Hz to 100 Hz. tanδ is defined as G″/G′.

Nanoindentation test: Nano-indentation tests were performed on Bioindenter UNHT^3 Bio (Anton Paar). The radius of the indenter (Ruby ball) was 0.5 mm. The samples were fixed on a flat glass slide by Loctite 406 glue in all tests. Normal load of 500 μN was chosen to test the samples.

Macroscopic indentation test: Macroscopic indentation tests were performed on adhesion testing machine (RTEC 2430, MFT-3000). The samples were fixed on a flat glass slide by Loctite 406 glue in all tests. For the sphere-to-disk test, a glass ball with a diameter of 5 mm was used as a contact pair. When the load was above 1 N, compression model of the electrical universal material testing machine with a 500 N load cell (EZ-Test, SHIMADZU, Japan) was used. All the test conditions are the same as the friction test.

The morphology characterization: The scanning electron microscope (SEM; Phenom ProX G5) and optical microscope Olympus BX51 were employed to observe the surface morphology of samples.

The friction characterization: The friction test was performed on conventional sphere-on-disk tribometer by recording the COF by using Tribometer (Anton Paar, Switzerland). A glass ball with a diameter of 5 mm was used as contact pair. The loads were selected as 1 mN to 20 N to evaluate its tribology performance and load-bearing capability. For load ranging from 1 mN to 1 N, the tribometer was Nano Tribometer, NTR^2, TTX; for load ranging from 1 N to 20 N, the tribometer was Tribometer, TRB. The calculation of all COFs was conducted in a reciprocating mode using the tribometer software. The COFs were calculated as the ratio of friction force to the applied normal load. We halted the friction test when we noticed a pronounced rise in frictional force in the sample, stemming from deformation hysteresis. This precaution was taken to prevent excessive frictional forces from exceeding the range of the friction machine's sensor, which could damage the instrument.

The ATR-FTIR characterization: A Nicolet iS10 (Thermo Scientific, USA) Fourier transform infrared spectrometer was used to confirm the components of hydrogel and polymer brush.

Contact angle characterization: Contact angles of samples were determined by using DSA-100 optical contact angle meter (Kruss Company, Ltd., Germany).

3 Results and discussion

In order to explore the influence of load-bearing capacity on surface friction behavior of cartilage-inspired hydrogel, the two-layer design strategy was adopted. The interface contribution in friction can be controlled by using a hydrated polymer brush layer as surface top layer while the moduli of bottom hydrogel matrix were finely regulated to adjust the load-bearing capacities and deformation/hysteresis contribution in our system. Specifically, a MTH was synthesized by our previous method as bottom hydrogel matrix [25], while hydrated polyelectrolyte brush chains interpenetrating the subsurface of hydrogel matrix was covalently anchored on MTH, so as to generate a cartilage-inspired bilayer modulus tunable hydrogel (BMTH). Figure 2 showed the preparation process for MTH and BMTH. Firstly, P(AAc-co-HEMA-Br) hydrogel was synthesized by UV copolymerization of the precursor solution mainly containing acrylic acid (AAc), 2-hydroxyethyl methacrylate-bromine (HEMA-Br). After polymerization, this hydrogel was immersed in calcium acetate (CaAc) solution to form a PAAc-CaAc network to become MTH. Subsequently, the P(AAc-CaAc-co-HEMA-Br) hydrogel (MTH) was immersed into the reaction solution containing monomer 3-sulfopropyl methacrylate potassium (SPMA) to perform atom transfer radical polymerization (ATRP) for generating surface polyelectrolyte brush chains (PSPMA) interpenetrated hydration layer to obtain the bilayer modulus tunable hydrogel (BMTH). To regulate the moduli of MTH and BMTH, samples are immersed in CaAc solutions with different concentrations. As shown in Fig. 2, P(AAc-CaAc-co- HEMA-Br)-B-Soft (BMTH-Soft) was successfully prepared by applying low concentration CaAc (250 mM) to form a loose PAAc-CaAc network, while P(AAc-CaAc-co-HEMA-Br)-B-Hard (BMTH-Hard) was obtained by immersing BMTH-Soft in high concentration CaAc solution for forming a denser PAAc-CaAc network. MTHs with different moduli were prepared as the same procedure. The mechanism for concentrations-dependent moduli change of MTH and BMTH was the strategy of enhancing the electrostatic interaction in hydrophobic media [39]. In detail, the hydrophobic residues (acetate) in hydrogel network of MTH and BMTH formed hydrophobic regions and remarkably reduced the local permittivity of the media, resulting in the enhancement of the

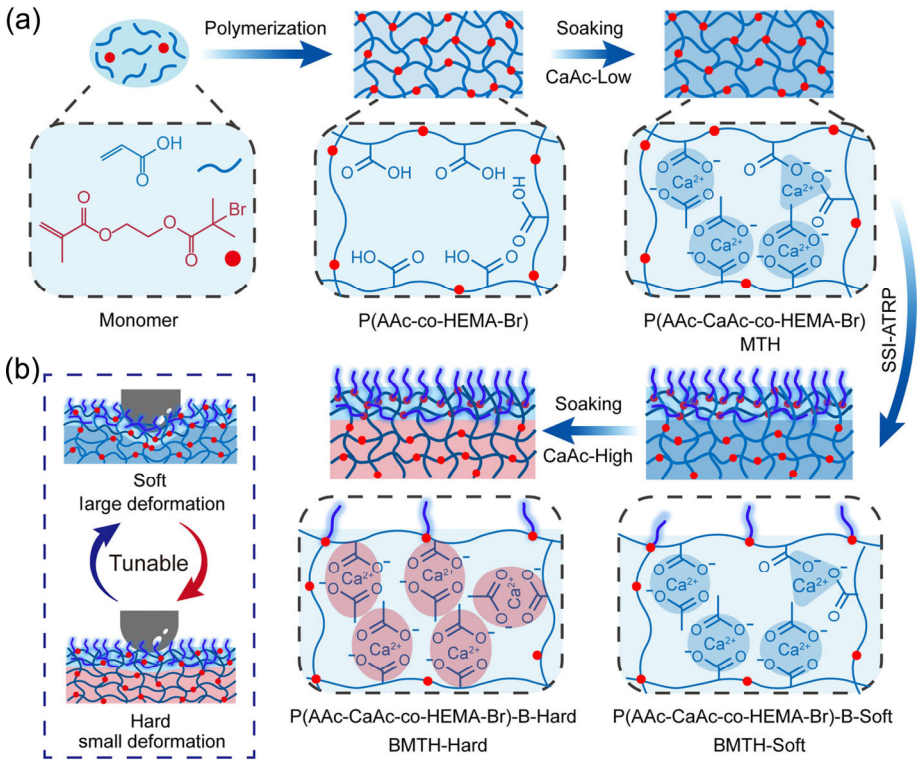

Fig. 2 (a) Schematic illustration for the preparation of MTH, BMTH, and the modulus tuning mechanism. The blue filled area represents ionic interaction, the red filled area represent the cooperative effects of hydrophobic interaction and the enhanced ionic interaction. (b) Schematic illustration of the deformation difference between hydrogels under load.

electrostatic interaction of the nearby charged residues (Ca^{2+}–COO^{-}) to induce moduli change [39, 44]. The moduli change of the hydrogel matrix would lead to a great difference in the interface contact states when bearing load (Fig. 2(b)). The surface hydration effect of BMTH was almost kept unchanged because of the branched polyelectrolyte chains with highly hydrated sulfonate ions in the top interpenetrating layer. Therefore, the main difference among BMTH samples was the load-bearing capacities of the hydrogel matrix.

Based on the CaAc solubility, concentrations were selected from 250 mM to 1,400 mM (saturated). The surface morphology of MTH and BMTH was characterized by SEM and the corresponding energy dispersive spectroscopy (EDS) test was also applied to verify the successful graft of polymer brush lubrication layer (Fig. 3(a)). Compared to MTHs, the surface of BMTHs exhibited regular wrinkle patterns with clear gaps resulting from the high grafting density of polymer brush. In addition, the cross-section characterization showed that polymer brush layer was perfectly bonded. The cross-section SEM and EDS test of the BMTHs show that the top surface layer has high sulfur content from PSPMA and the bulk phase has high carbon content from PAAc. The calcium ions will cross-link sulfonate ions through electrostatic interaction, resulting in differences in surface morphology. However, within our concentration range, there is little difference in surface morphology between the samples soaked with the lowest concentration (250 mM) and those soaked with the highest concentration (1,400 mM). It is probable that calcium ions are sufficiently cross-linked for SPMA in our experiment, and surface cross-linking and morphology are not sensitive to concentration changes.

The thickness of the surface lubrication layer can be controlled by controlling the ATRP grafting time. In Fig. 3(b), the thickness of PSPMA polymer brush layer increased with the extension of the grafting time in ATRP process, while it leveled off after 40 min reaction (~250 μm) [9, 16]. BMTHs with a moderate thickness (~250 μm) was selected for follow-up experiments. The thickness of polymer brush layer

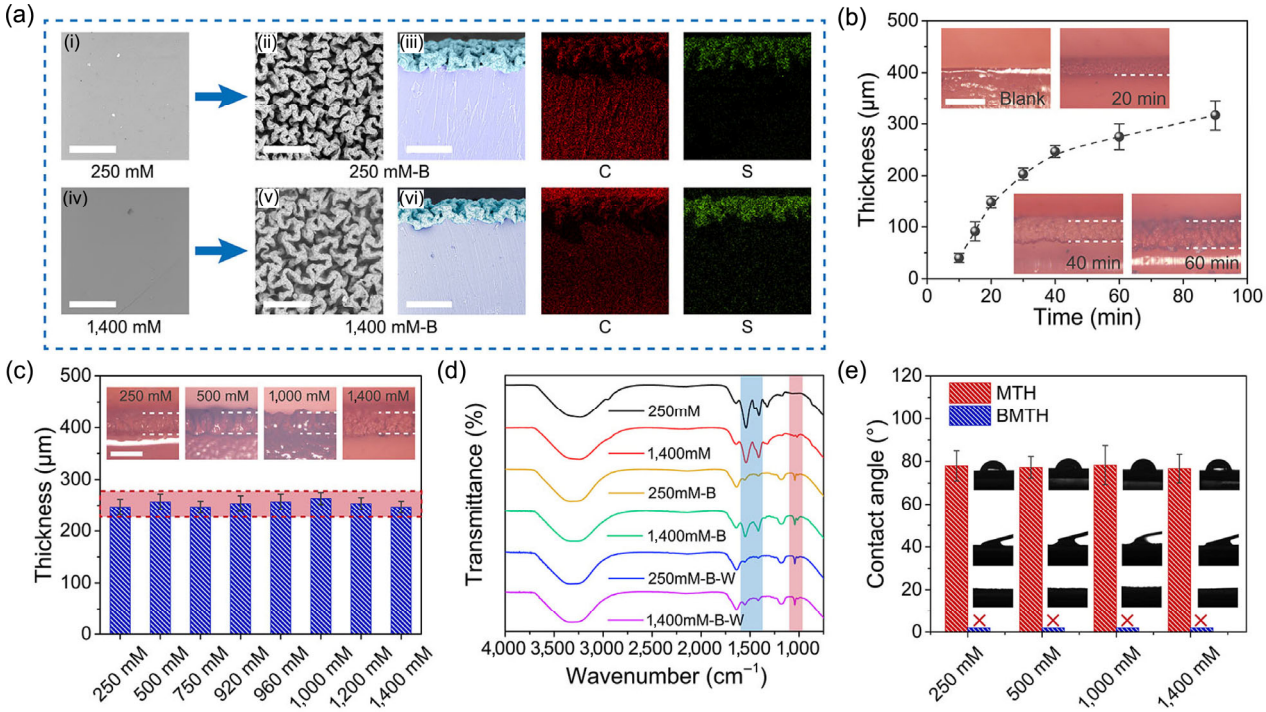

Fig. 3 (a) SEM images showing the surface morphology of (i) MTH, (ii) BMTH soaking in 250 mM CaAc (scale bar: 200 μm) and (iii) the corresponding cross-section morphology of BMTH and EDS results (scale bar: 200 μm); (iv–vi) corresponding results of samples soaking in 1,400 mM CaAc. (b) The relationship between lubricating layer thickness and grafting time of polymer brush in swelling state(scale bar: 400 μm). (c) The relationship between lubricating layer thickness and CaAc concentrations; grafting time: 40 min (scale bar: 400 μm). (d) ATR-FTIR spectra of MTHs and BMTHs immersed in 250 mM and 1,400 mM CaAc solution and the BMTHs rinsed by water. (e) Contact angles of MTHs and BMTHs immersed in different CaAc solutions.

remained almost unchanged after soaking into CaAc solution with different concentrations to obtain corresponding BMTH (Fig. 3(c)). This means that the thickness of top layer was also not sensitive to concentration changes.

ATR-FTIR was also employed to analyze the surface properties of samples. Compared with the MTHs, the peak at ~1,050 cm^{-1} for BMTHs was attributed to the stretching vibration of the sulfur–oxygen double bond, indicating the successful grafting of PSPMA polymer brush (Fig. 3(d)). The samples immersed in different CaAc concentrations exhibited different peak signals at ~1,420 cm^{-1} and ~1,540 cm^{-1}. After the growth of the polymer brush, these CaAc peak signals were weakened. Although the polymer brush layer also showed an obvious CaAc signals at high concentration (1,400 mM), these signals were decreased to be the same as the 250 mM when the polymer brush layer was rinsed with water. EDS results also showed that the surface chemical composition of polymer brush layers was similar after being rinsed with water (Fig. S1 in the Electronic Supplementary Material (ESM)). In addition, the contact angles of MTHs and BMTHs treated with different CaAc solutions also showed no differences. After grafting polymer brush layer, the surface of the hydrogel matrix became super-hydrophilic, and the water droplet spread instantly upon contact with this layer (Fig. 3(e)). These results showed that the properties of the surface polymer brush layer in BMTH were similar in the water-lubricated environment and the polymer brush layer properties were insensitive to CaAc concentration in this experiment.

The sensitivity of bulk phase mechanical properties of MTHs and BMTHs hydrogels to CaAc concentration was characterized by tensile testing and nanoindentation. First, a tensile test was applied to verify the modulus differences among these as-prepared hydrogels. As shown in Fig. 4(a), the modulus and strength of hydrogel matrix increased with the rise of the CaAc concentrations, which was attributed to the denser PAAc-CaAc network

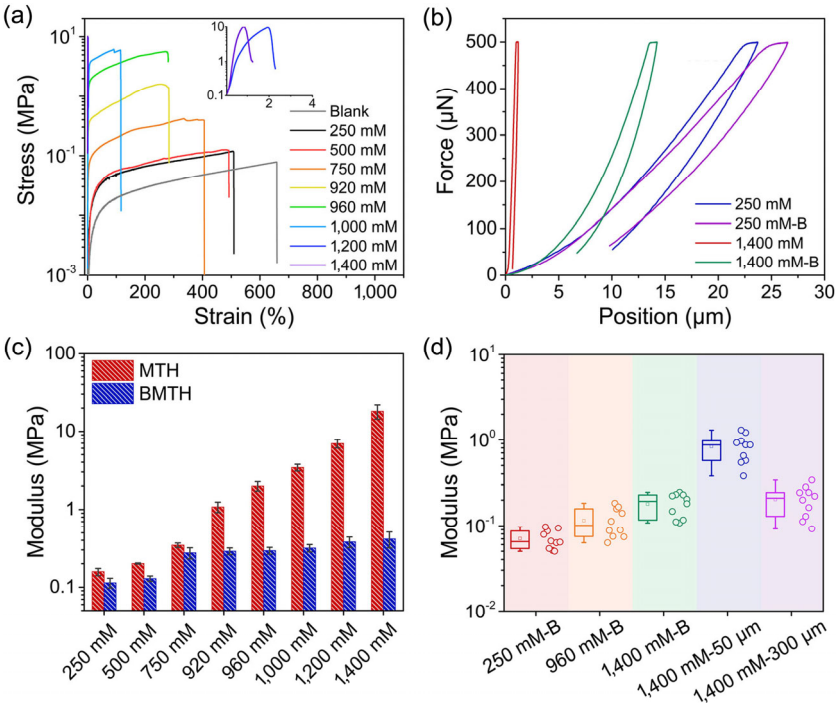

Fig. 4 (a) Tensile test of MTH soaking in different CaAc solotions. (b, c) Force-position curves and modulus of nano-indentation tests for MTHs and BMTHs immersed in different CaAc solutions. (d) Modulus results of nano-indentation tests for BMTHs immersed in different CaAc solutions. And the BMTHs immersed in 1,400 mM CaAc solution with different thickness.

formed within the matrix. Although hydrogels with N-isopropylacrylamide (NIPAAM) cause phase separation and modulus shifts with temperature changes. NIPAAM's significant volume changes can alter the grafting density of surface brushes, adding experimental variables. Hence, we opted for the PAAc-CaAc system with minimal volume alterations. The effect of salt concentration on the surface layer modulus is also investigated. According to the results of nano-indentation test (Figs. 4(b) and 4(c)), the surface modulus of MTH matrix was decreased after grafting PSPMA polymer brush layer. The moduli results of MTHs soaked in different CaAc solutions were corresponded with the tensile test. Meanwhile, due to the substrate effect and calcium ions crosslinking sulfonate ions, the moduli test results of polymer brush layers increased with the rise of the moduli for MTH matrixes slightly. However, this effect was negligible when compared with the obvious increase of whole modulus of BMTH. Furthermore, the accurate surface modulus of the top polymer brush layer was obtained by testing its cross section surface to minimize the substrate effect (Fig. 4(d)). The surface layer modulus of tested from the cross section is slightly lower than that of the direct surface test. The surface moduli of the top layer with different thicknesses were also tested. It was found that the thinner the layer, the stronger the substrate effect. Therefore, based on the surface and bulk phase characterizations, MTHs and BMTHs can be used as model materials to detect the effect of load-bearing capacities on friction.

Subsequently, the surface friction behavior of MTHs and BMTHs were investigated by employing a sphere-to-disk contact mode with reciprocating sliding test (Figs. 5(a) and 5(b)). When increasing the normal load, the COFs of both MTHs and BMTHs decreased first and then increased. The COFs of BMTHs were much lower than that of MTHs. The higher the modulus of the bulk phase was, the lower the COF was. The normal displacements under different normal loads were tested by macroscopic indentation and presented in Figs. 5(c) and 5(d). Compared with the displacements of MTHs, those of BMTHs were larger at low normal load. However, as the load increased, this difference gradually decreased. Correspondingly, it was found that this trend was more obvious with increasing the modulus

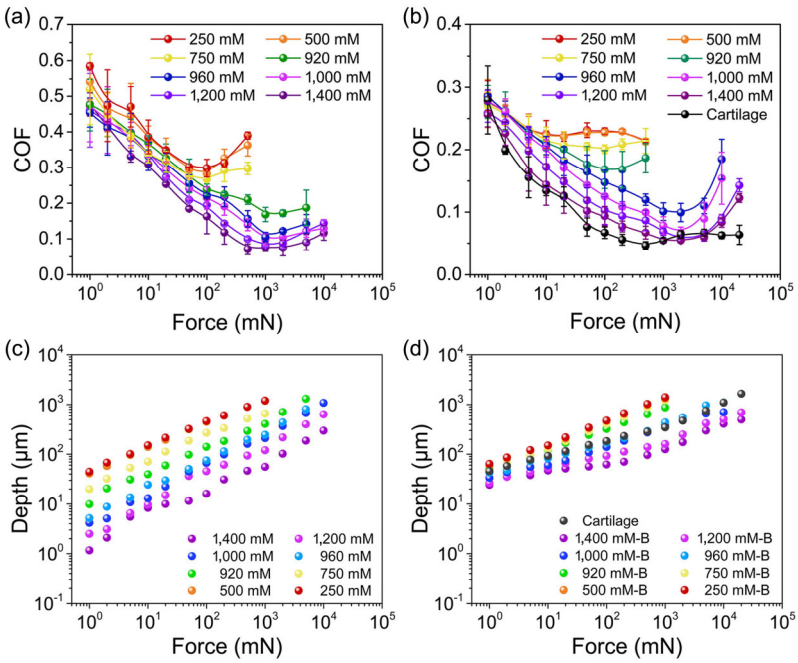

Fig. 5 COFs of (a) MTHs and (b) BMTHs and cartilage under different normal forces. Normal displacement of (c) MTHs and (d) BMTHs immersed in different CaAc solutions and cartilage under different normal forces.

of hydrogel matrix. This phenomenon was attributed to the low modulus of polymer brush layer and the high modulus of hydrogel matrix. Soft polymer brush layer would deform largely even under a small load, while the hard hydrogel matrix would bear the normal pressure under a harsh load. The deformation of hard MTHs and BMTHs under loading was much smaller than that of soft MTHs and BMTHs in contact. Meanwhile, the indentation displacement of natural cattle cartilage was also tested as control, and it was found that the trend of cartilage was the same as that of BMTHs because of the gradient structure itself. According to the two-term non-interacting model, COF (μ), was the sum of interfacial component (μ_{Int}), and deformation/hysteresis component (μ_{Hyst}) [25–28]:

$$\mu = \mu_{\text{Int}} + \mu_{\text{Hyst}} \tag{1}$$

When the normal load was small, the mechanical deformation of the hydrogel was not obvious, the COF (μ) was mainly determined by interfacial component μ_{Int}. The polymer brush layer can effectively reduce the surface contribution (μ_{Int}) and reduce the coefficient of friction. With the increasing of normal load, the mechanical deformation of hydrogel was not negligible, while the contribution of deformation component (μ_{Hyst}) was dominant in the whole sliding process. The stiff hydrogel matrix would greatly reduce the deformation/hysteresis (μ_{Hyst}) during friction (Fig. 6(a)).

Furthermore, the applied normal loads were transformed into normal stress (Fig. 6(b)) [45]. Interestingly, the COFs values of BMTHs with different load-bearing capacities concentrated in a narrow area while that of MTHs spread over a large area. According to the elastomer friction theory developed by Moore [23, 28], the μ_{Int} contributed by interface term was defined as

$$\mu_{\text{Int}} \sim \frac{E}{P^r}\tan\delta \tag{2}$$

While the μ_{Hyst} contributed by deformation/hysteresis term was

$$\mu_{\text{Hyst}} \sim \left(\frac{P}{E}\right)^n \tan\delta \tag{3}$$

According to Eqs. (2) and (3), both modulus and damping factor played an important role in COFs. The modulus results E and damping factor results $\tan\delta$ were showed in Fig. S2 in the ESM. The network modulus of MTH hydrogel matrix increased with

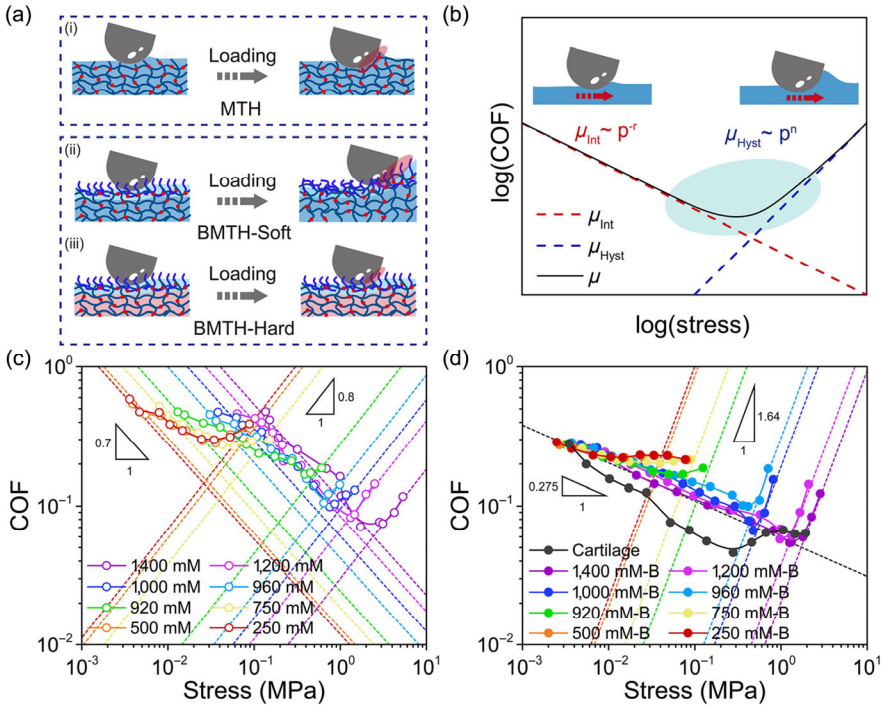

Fig. 6 (a) Schematic diagram showing the friction state of MTH and BMTH. (b) Schematic diagram and the scaling analysis of the interface and deformation/hysteresis contribution to COF. (c, d) COFs and scaling analysis of MTH and BMTH immersed in different CaAc solutions and cartilage under different normal stress.

extending the treatment concentration of CaAc solution, but the damping factor first increased and then decreased. Specifically, the moduli of hydrogel matrix varies from ~0.15 MPa to ~18 MPa, about two orders of magnitude, while the damping factors varies from ~0.1 to ~0.95 at testing condition, about one order of magnitude. Therefore, in the current research system, the differences of COFs were mainly caused by the moduli. Based on this hypothesis, these COF formulas above were simplified and became μ_{Int}~P^{-r} and μ_{Hyst}~P^{n}. This theory well explained the evolution trend of μ ($\mu = \mu_{Int} + \mu_{Hyst}$). When the normal stress P was small, the contribution of μ_{Int} was greater than that of μ_{Hyst}, so COFs decreased with increasing the normal stress. Furthermore, when the normal stress continued to increase, the mechanical deformation of the material would become large enough so that the effect of deformation cannot be ignored. Correspondingly, the contribution of μ_{Hyst} would exceed that of μ_{Int}, and the COFs would increase with the rising of normal stress. This went a long way towards explaining the trend in COFs. In this system of study, it was found that the r in interface contribution of COF for MTHs was ~0.7 and the n in deformation/hysteresis contribution of COF for MTHs was ~0.8 by fitting the trend (Fig. 6(c)). The r in interface contribution of COF for BMTHs was ~0.275 and the n in deformation/hysteresis contribution of COF for BMTHs was ~1.64 (Fig. 6(d)). Interestingly, the values of COF of BMTHs were very similar in the interface domain while those of MTHs are different. According to the theory mentioned above, this phenomenon was attributed to the difference between polymer brush modulus and hydrogel matrix modulus. For the sample without polymer brush layer, the modulus term E in μ_{Int} was the same as that in μ_{Hyst}, leading to this difference. However, the modulus term in μ_{Int} was different from that in μ_{Hyst} for BMTH. The surface moduli of the polymer brush were almost the same while the moduli of the hydrogel matrix in BMTHs were different. The hydrated soft polymer brush surface, with similar chemical properties (Fig. 3), contributes uniformly. As a result, it dissipated and reduced the contact stress, making deformation at low loads similar. Thus, at low stresses, the COF was determined by the modulus of the polymer brush, resulting in similar contribution of interface COFs of BMTHs. The cartilage curve diverged from the

normal curve. Different from the bilayer hydrogel, this continuously gradient modulus of cartilage might cause this deviation from our hydrogel curve.

Based on the above results, higher load-bearing capacity results in lower COF in bilayer hydrogel. Meanwhile, the hydrated polymer brush layer also played an important role in reducing the interface COF. MTHs and BMTHs with high mechanical strengths obtained by treatment in 1,400 mM CaAc solution were used for detecting the dissipation and anti-wear performance of polymer brush layer. At first, the effects of sliding frequencies on the COFs of MTH and BMTH were investigated. As illustrated in Fig. S3 in the ESM, the COFs of the MTH decreased first and then increased with the rising of sliding frequencies unstably. By contrast, the COFs of BMTH were stable and only showed a little decrease with increasing the sliding frequencies, indicating the presence of the polymer brush layer could form a stable lubrication layer to reduce the noise of interface friction. The thickness of soft polymer brush layer also has a great influence on the COF and wear resistance property. Subsequently, the samples were conducted for 36,000 friction cycles under normal load of 1 N. It was found that the appropriate thickness of the top polymer brush layer was also the key responsible for both COF and wear resistance of BMTH (Figs. 7(a) and 7(b)). If the polymer brush layer is very thin (100 μm), the interface contact stress would be large and the lubrication layer is easy to wear, resulting from the rising apparent modulus by substrate effect as well as the large contact pressure (Fig. 7(c)). If this layer is thick (300 μm), it would arise viscous resistance and deformation hysteresis, leading to an increase of the interface COF and an improvement in wear resistance. The COF would decrease slightly when the thick layer (300 μm) was worn away gradually, and the viscous resistance and deformation hysteresis were suppressed. For the comparison among MTH, BMTH and cartilage under normal load of 1 N, the COF of MTH was ~0.1 but a sudden surge appeared subsequently. By contrast, the COF of BMTH was always maintained at a stable and low level (~0.05), indicating the excellent robustness

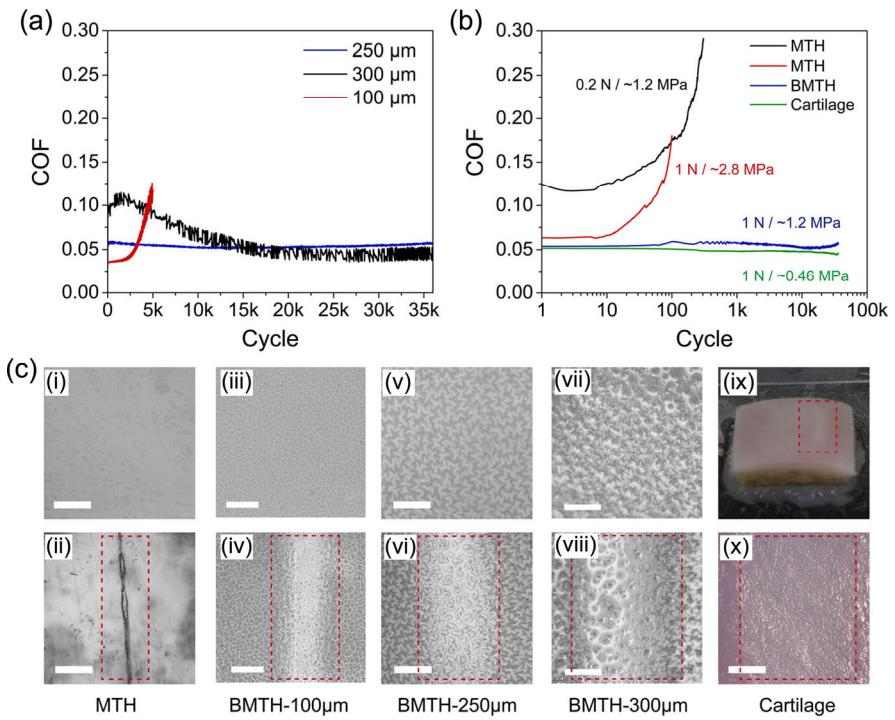

Fig. 7 (a) Evolution of COF with time for BMTH with different polymer brush layer thickness (applied load: 1 N, 1 Hz) for 36,000 friction cycles. (b) Evolution of COF with time for MTH and BMTH (applied load: 1 N, 1 Hz) for 36,000 friction cycles. (c) The optical micrographs of worn scars: MTH (i) before and (ii) after encountering ~100 sliding cycles, BMTH-100 μm (iii) before and (iv) after encountering ~4,000 sliding cycles, (v, vi) BMTH-250 μm, (vii, viii) BMTH-300 μm, and (ix, x) cartilage before and after encountering 36,000 sliding cycles (scale bar: 400 μm).

and wear-resistance of polymer brush layer under the continuous shearing/loading condition. Taking the dissipation of polymer brush into consideration, MTH was also applied by 0.2 N for normal stress ~1.2 MPa, and it still exhibited a sudden surge of COF within 100 cycles. It was observed that the surface of MTH appeared obvious wear scars after only encountering 100 sliding cycles under the normal load of 1 N. By contrast, there was no obvious wear appeared on the surface of BMTH after even encountering 36,000 sliding cycles. This showed the excellent synergistic effect of interfacial hydration and dissipative stress of polymer brush layer. High modulus gradients between surface and substrate can cause stress mismatches and reduce wear resistance. Our *in-situ* growing polymer brushes interpenetrate on the surface and Figs. 4(c) and 4(d) showed that substrate effect increased their moduli. The soft interpenetrating layer at the brush–substrate interface might decrease this gradient and improve wear resistance. Finally, the lubrication performance and wear-resistance of natural cartilage were also evaluated as a comparison with BMTH. The natural articular cartilage showed low COF and good abrasion resistance. There was no wear debris appeared on cartilage surface while the width of the abrasion was wider than the BMTH. The COF of BMTH was almost similar to natural cartilage at the same loading condition due to the hydrated surface and gradient high load-bearing matrix. The natural cartilage exhibited a better anti-wear performance and a wider abrasion than those of the BMTH, which may be mainly due to the special stress dissipation mechanism from its continuously gradient modulus.

4 Conclusions

In this work, a bilayer modulus tunable hydrogel (BMTH) as novel cartilage prototype consisting of a top thick polymer brush interpenetrating layer and a bottom matrix with tunable moduli was designed to reveal the effect of mechanical modulus and load-bearing capacity on lubrication behavior. Compared with the bare modulus tunable hydrogel (MTH), the top soft layer endowed BMTH with excellent stress dissipation, hydration lubrication, and anti-wear properties, reducing the interface interaction contribution (μ_{Int}) in friction process. The moduli tunable matrix provided an adjustable load-bearing capacity for BMTH to investigate the contribution of deformation (μ_{Hyst}) to COFs systematically. High load-bearing capacity reduces friction by suppressing deformation hysteresis (μ_{Hyst}). The optimized BMTH can present a stable and low COF (~0.05) during the 36,000 sliding cycles, comparable to natural cartilage. This result indicates the low COF and robust lubrication of hydrogel-based cartilage prototypes are highly related to synergistic effect of interfacial hydration and load-bearing capacity under the continuous shearing/loading conditions. This research provides a basic design principle for preparing cartilage-like hydrogels soft materials with low friction, high load-bearing capacity, and considerable durability.

Acknowledgements

We are grateful for financial support from National Natural Science Foundation of China (22032006, 52075522, 52322506), Strategic Priority Research Program of the Chinese Academy of Sciences (XDB 0470201), Outstanding Youth Fund of Gansu Province (21JR7RA095), Key Research Project of Shandong Provincial Natural Science Foundation (ZR2021ZD27), Gansu Province Basic Research Innovation Group Project (22JR5RA093), West Light Foundation of The Chinese Academy of Sciences (xbzg-zdsys-202211).

Declaration of competing interest

The authors have no competing interests to declare that are relevant to the content of this article. The author Shuanhong MA is the Youth Editorial Board Member of this journal. The author Feng ZHOU is the Editorial Board Member of this journal.

Electronic Supplementary Material Supplementary material is available in the online version of this article at https://doi.org/10.1007/s40544-023-0846-3.

References

[1] Lin W F, Kluzek M, Iuster N, Shimoni E, Kampf N, Goldberg

R, Klein J. Cartilage-inspired, lipid-based boundary-lubricated hydrogels. *Science* **370**(6514): 335–338 (2020)

[2] Forster H, Fisher J. The influence of loading time and lubricant on the friction of articular cartilage. *Proc Inst Mech Eng H* **210**(2): 109–119 (1996)

[3] Lin, W F, Klein J. Recent progress in cartilage lubrication. *Adv Mater***33**: 2005513 (2021)

[4] Klein J. Hydration lubrication. *Friction* **1**(1): 1–23 (2013)

[5] Greene G W, Banquy X, Lee D W, Lowrey D D, Yu J, Israelachvili J N. Adaptive mechanically controlled lubrication mechanism found in articular joints. *Proc Natl Acad Sci U S A* **108**(13): 5255–5259 (2011)

[6] Mow V C, Ateshian G A, Spilker R L. Biomechanics of diarthrodial joints: A review of twenty years of progress. *J Biomech Eng* **115**(4B): 460–467 (1993)

[7] Mow V C, Kuei S C, Lai W M, Armstrong C G. Biphasic creep and stress relaxation of articular cartilage in compression: Theory and experiments. *J Biomech Eng* **102**(1): 73–84 (1980)

[8] Mow V C, Guo X E. Mechano-electrochemical properties of articular cartilage: Their inhomogeneities and anisotropies. *Annu Rev Biomed Eng* **4**: 175–209 (2002)

[9] Rong M M, Liu H, Scaraggi M, Bai Y Y, Bao L Y, Ma S H, Ma Z F, Cai M R, Dini D, Zhou F. High lubricity meets load capacity: Cartilage mimicking bilayer structure by brushing up stiff hydrogels from subsurface. *Adv Funct Materials* **30**(39): 2004062 (2020)

[10] Antons J, Marascio M G M, Nohava J, Martin R, Applegate L A, Bourban P E, Pioletti D P. Zone-dependent mechanical properties of human articular cartilage obtained by indentation measurements. *J Mater Sci Mater Med* **29**(5): 57 (2018)

[11] Zhao X H, Chen X Y, Yuk H, Lin S T, Liu X Y, Parada G. Soft materials by design: Unconventional polymer networks give extreme properties. *Chem Rev* **121**(8): 4309–4372 (2021)

[12] Gong J P, Kurokawa T, Narita T, Kagata G, Osada Y, Nishimura G, Kinjo M. Synthesis of hydrogels with extremely low surface friction. *J Am Chem Soc* **123**(23): 5582–5583 (2001)

[13] Tse J R, Engler A J. Preparation of hydrogel substrates with tunable mechanical properties. *CP Cell Biology* **47**(1): https://doi.org/10.1002/0471143030.cb1016s47 (2010)

[14] Duque-Ossa L C, Ruiz-Pulido G, Medina D I. Triborheological study under physiological conditions of PVA hydrogel/HA lubricant as synthetic system for soft tissue replacement. *Polymers* **13**(5): 746 (2021)

[15] Liu J, Lin S T, Liu X Y, Qin Z, Yang Y Y, Zang J F, Zhao X H. Fatigue-resistant adhesion of hydrogels. *Nat Commun* **11**: 1071 (2020)

[16] Liu H, Zhao X D, Zhang Y L, Ma S H, Ma Z F, Pei X W, Cai M R, Zhou F. Cartilage mimics adaptive lubrication. *ACS Appl Mater Interfaces* **12**(45): 51114–51121 (2020)

[17] Chen M, Briscoe W H, Armes S P, Klein J. Lubrication at physiological pressures by polyzwitterionic brushes. *Science* **323**(5922): 1698–1701 (2009)

[18] Chen K, Zhang D K, Cui X T, Wang Q L. Research on swing friction lubrication mechanisms and the fluid load support characteristics of PVA–HA composite hydrogel. *Tribol Int* **90**: 412–419 (2015)

[19] Wu X F, Li W, Chen K, Zhang D K, Xu L M, Yang X H. A tough PVA/HA/COL composite hydrogel with simple process and excellent mechanical properties. *Mater Today Commun* **21**: 100702 (2019)

[20] Ohsedo Y, Takashina R, Gong J P, Osada Y. Surface friction of hydrogels with well-defined polyelectrolyte brushes. *Langmuir* **20**(16): 6549–6555 (2004)

[21] Fan Y H, Zhou G Y, Zhang G T, Li F. Comparative study on the mechanical behavior of the interface between natural cartilage and artificial cartilage. *Soft Mater* **19**(4): 400–419 (2021)

[22] Yang F C, Zhao J C, Koshut W J, Watt J, Riboh J C, Gall K, Wiley B J. A synthetic hydrogel composite with the mechanical behavior and durability of cartilage. *Adv Funct Materials* **30**(36): 2003451 (2020)

[23] Greenwood J A, Tabor D. The friction of hard sliders on lubricated rubber: The importance of deformation losses. *Proc Phys Soc* **71**(6): 989–1001 (1958)

[24] Gong J P, Katsuyama Y, Kurokawa T, Osada Y. Double-network hydrogels with extremely high mechanical strength. *Adv Mater* **15**(14): 1155–1158 (2003)

[25] Zhang Y L, Zhao W Y, Ma S H, Liu H, Wang X W, Zhao X D, Yu B, Cai M R, Zhou F. Modulus adaptive lubricating prototype inspired by instant muscle hardening mechanism of catfish skin. *Nat Commun* **13**(1): 377 (2022)

[26] Persson B N J. Theory of rubber friction and contact mechanics. *J Chem Phys* **115**(8): 3840–3861 (2001)

[27] Derjaguin B V, Muller V M, Toporov Y P. Effect of contact deformations on the adhesion of particles. *J Colloid Interface Sci* **53**(2): 314–326 (1975)

[28] Adams M J, Briscoe B J, Johnson S A. Friction and lubrication of human skin. *Tribol Lett* **26**(3): 239–253 (2007)

[29] Lin P, Ma S H, Wang X L, Zhou F. Molecularly engineered dual-crosslinked hydrogel with ultrahigh mechanical strength, toughness, and good self-recovery. *Adv Mater* **27**(12): 2054–2059 (2015)

[30] Sun J Y, Zhao X H, Illeperuma W R K, Chaudhuri O, Oh K H, Mooney D J, Vlassak J J, Suo Z G. Highly stretchable and tough hydrogels. *Nature* **489**(7414): 133–136 (2012)

[31] Hua M T, Wu S W, Ma Y F, Zhao Y S, Chen Z L, Frenkel I, Strzalka J, Zhou H, Zhu X Y, He X M. Strong tough hydrogels via the synergy of freeze-casting and salting out. *Nature* **590**: 594–599 (2021)

[32] Wu S W, Hua M T, Alsaid Y, Du Y J, Ma Y F, Zhao Y S, Lo C, Wang C, Wu D, Yao B W, et al. Poly(vinyl alcohol) hydrogels with broad-range tunable mechanical properties via the hofmeister effect. *Adv Mater***33**: 2007829 (2021)

[33] Matsuda T, Kawakami R, Namba R, Nakajima T, Gong J P. Mechanoresponsive self-growing hydrogels inspired by muscle training. *Science* **363**(6426): 504–508 (2019)

[34] Lin S T, Liu X Y, Liu J, Yuk H, Loh H, Parada G A, Settens C, Song J, Masic A, Mckinley G, et al. Anti-fatigue-fracture hydrogels. *Sci Adv* **5**(1): eaau8528 (2019)

[35] Zheng Y, Kiyama R, Matsuda T, Cui K P, Li X Y, Cui W, Guo Y Z, Nakajima T, Kurokawa T, Gong J P. Nanophase separation in immiscible double network elastomers induces synergetic strengthening, toughening, and fatigue resistance. *Chem Mater* **33**(9): 3321–3334 (2021)

[36] Sedlačík T, Nonoyama T, Guo H L, Kiyama R, Nakajima T, Takeda Y, Kurokawa T, Gong J P. Preparation of tough double- and triple-network supermacroporous hydrogels through repeated cryogelation. *Chem Mater* **32**(19): 8576–8586 (2020)

[37] Sun T L, Kurokawa T, Kuroda S, Bin Ihsan A, Akasaki T, Sato K, Haque M A, Nakajima T, Gong J P. Physical hydrogels composed of polyampholytes demonstrate high toughness and viscoelasticity. *Nature Mater* **12**(10): 932–937 (2013)

[38] Wang Z, Zheng X J, Ouchi T, Kouznetsova T B, Beech H K, Av-Ron S, Matsuda T, Bowser B H, Wang S, Johnson J A, *et al*. Toughening hydrogels through force-triggered chemical reactions that lengthen polymer strands. *Science* **374**(6564): 193–196 (2021)

[39] Nonoyama T, Lee Y W, Ota K, Fujioka K, Hong W, Gong J P. Instant thermal switching from soft hydrogel to rigid plastics inspired by thermophile proteins. *Adv Mater* **32**(4): 1905878 (2020)

[40] Zhang X Y, Lou Z C, Yang X H, Chen Q, Chen K, Feng C N, Qi J W, Luo Y, Zhang D K. Fabrication and characterization of a multilayer hydrogel as a candidate for artificial cartilage. *ACS Appl Polym Mater* **3**(10): 5039–5050 (2021)

[41] Lin P, Zhang R, Wang X L, Cai M R, Yang J, Yu B, Zhou F. Articular cartilage inspired bilayer tough hydrogel prepared by interfacial modulated polymerization showing excellent combination of high load-bearing and low friction performance. *ACS Macro Lett* **5**(11): 1191–1195 (2016)

[42] Qu M H, Liu H, Yan C Y, Ma S H, Cai M R, Ma Z F, Zhou F. Layered hydrogel with controllable surface dissociation for durable lubrication. *Chem Mater* **32**(18): 7805–7813 (2020)

[43] Wu B Q, Feng E L, Liao Y M, Liu H W, Tang R Z, Tan Y. Brush-modified hydrogels: Preparations, properties, and applications. *Chem Mater* **34**(14): 6210–6231 (2022)

[44] Linse P, Lobaskin V. Electrostatic attraction and phase separation in solutions of like-charged colloidal particles. *Phys Rev Lett* **83**(20): 4208–4211 (1999)

[45] Popov V L. Contact mechanics and friction. Springer, 2010.

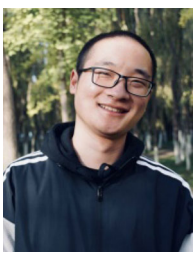

Yunlei ZHANG. He received his B.S. degree from Northwest Normal University, China, in 2018. He graduated and obtained his Ph.D. degree from the Lanzhou Institute of Chemical Physics (LICP), Chinese Academy of Sciences (CAS) in 2023. He is currently a postdoctoral researcher at RIKEN Center for Emergent Matter Science (CEMS). His research mainly focuses on the friction, adhesion, and lubrication of soft materials such as supramolecular polymers and gels.

Shuanhong MA. He received his B.S. in Tianshui Normal University, China, in 2011. He got his Ph.D. degree in LICP, CAS, in 2016. He is currently a professor of State Key Laboratory of Solid Lubrication, LICP, CAS. He has published over 90 papers (e.g., *Nat Commun*, *PNAS*, *Matter*), obtained more than 20 patents for invention, and received nearly 3,000 citations. His current research interests focus on the mechanics of soft contact interface, lubrication modification & friction control.

Feng ZHOU. He got his Ph.D. degree in 2004 in LICP, CAS. He spent three years (2005–2008) in the Department of Chemistry, University of Cambridge, UK, as a postdoctoral research associate. He is currently a professor and director of State Key Laboratory of Solid Lubrication, LICP, CAS. He has published over 500 papers (e.g., *Nat Commun, Sci Adv, PNAS, Matter*), obtained more than 160 patents for invention, and received over 20,000 citations. His research interests are surfaces/interfaces of soft matters, functional wet/slippery coatings, and friction control.